Forward-Scattering Analysis in a Focused-Beam System

Reuven Shavit, Tom Wells, and Albert Cohen

***Abstract*—The forward scattering from an arbitrarily shaped cylinder is characterized by its induced field ratio (IFR). This paper describes how a focused beam system is used to determine the scattering characteristics of an arbitrary-shaped cylinder. The fields of the transmitting and receiving antennas, as well as the scattered field from the cylinder, are described by equivalent fundamental Gaussian beams. An analytical procedure based on the computation of the coupling between the Gaussian beams in the focused beam system is used to determine the IFR of the cylinder. The results obtained by this method verify well with the scattering characteristics computed analytically or numerically by the method of moments or finite-elements method.**

***Index Terms*— Electromagnetic scattering, focused beams, Gaussian beams, radomes.**

I. Introduction

LARGE sandwich radomes are assembled from many panels connected together forming seams. These seams introduce scattering effects that degrade the overall electromagnetic performance of the antenna enclosed in the radome in terms of the transmission loss and radiation pattern. The knowledge of the scattering effect from an individual seam or for the same purpose an equivalent arbitrary-shaped cylinder is therefore the cornerstone of the entire scattering analysis. The scattering characteristics of an arbitrary-shaped cylinder is determined by its forward scattering value (IFR) and its scattering pattern. The IFR is defined as the ratio of the forward scattered field to the hypothetical field radiated in the forward direction by the plane wave in the reference aperture of width equal to the shadow of the geometrical cross section of the cylinder on the incident wavefront [1]. Low IFR is an indication of low scattering effect in the forward direction.

Analytical computations of the scattering characteristics from cylinders can be performed for canonical cross sections such as circular and ellipse, but for arbitrarily shaped cylinders this is a quite laborious and time consuming task which often requires intense numerical computations with techniques like method of moments or finite elements. Consequently, in many practical instances to speed up the developing process and verify the numerical computation, an accurate measurement technique of the IFR and the scattering pattern is required. Rusch [1] developed the IFR concept and suggested an experimental procedure to measure its value in the far-field for an arbitrarily shaped cylinder. This procedure lacks the capability to measure its scattering pattern. Shavit [2] proposed an alternate technique to determine both the IFR and the scattering patterns of an arbitrarily shaped cylinder based on near-field probing.

The current paper describes a new combined experimental and numerical procedure to determine the scattering characteristics of arbitrarily shaped cylinders using a focused-beam system. In the proposed system, the IFR is computed based on measurement data and the scattering pattern is directly measured in contrast to the method suggested in [2], which requires postprocessing of the measured data. The unique features of the focused-beam system avoid measurement errors due to specular and diffuse reflections from adjacent objects, in contrast to the existing errors in an open measurement system.

II. Method Description

The schematic configuration of the measurement system is shown in Fig. 1. The system is comprised of two circular identical dielectric lenses L_1 and L_2 with diameter D and two feed horns H_1 and H_2 with aperture dimensions $A * B$ and linear polarization. Each lens is designed to have two focal points located at distances f_1 and f_2 from the opposite sides of the lens surface. The actual distance of the feed horn phase center from the lens surface is d_1. In principle, it is desired $f_1 = d_1$; however, due to the movement of the feed horn phase center with frequency, this requirement is not perfectly achieved. The energy radiated by H_1 feed horn is captured by L_1 lens, focused to the common focal point of the L_1 and L_2 lenses, radiated into the L_2 lens, and focused again into the receiving H_2 feed horn. In such a system, most of the energy is transferred from one feed horn to the other feed horn without significant losses and reflection interference from surrounding objects. The x and z coordinates of the lens contours can be computed by geometrical optics and are described by [3]

$$x_{1,2} = \sqrt{(n^2-1)(z_{1,2}+t_{1,2})^2 + 2(n-1)f_{1,2}(x_{1,2}+t_{1,2})} \tag{1}$$

in which the subscripts 1, 2 designate the two opposite side contours of the lens, $t_{1,2}$ denote the lens thickness computed by

$$t_{1,2} = \frac{1}{n+1}\left[\sqrt{f_{1,2}^2 + \frac{(n+1)D^2}{4(n-1)}} - f_{1,2}\right] \tag{2}$$

Manuscript received February 24, 1997; revised November 18, 1997.

R. Shavit is with the Department of Electrical and Computer Engineering, Ben-Gurion University of the Negev, Beer Sheva 84105, Israel.

T. Wells and A. Cohen are with Electronic Space Systems Corp., Concord, MA 01742-4697 USA.

Publisher Item Identifier S 0018-926X(98)02684-2.

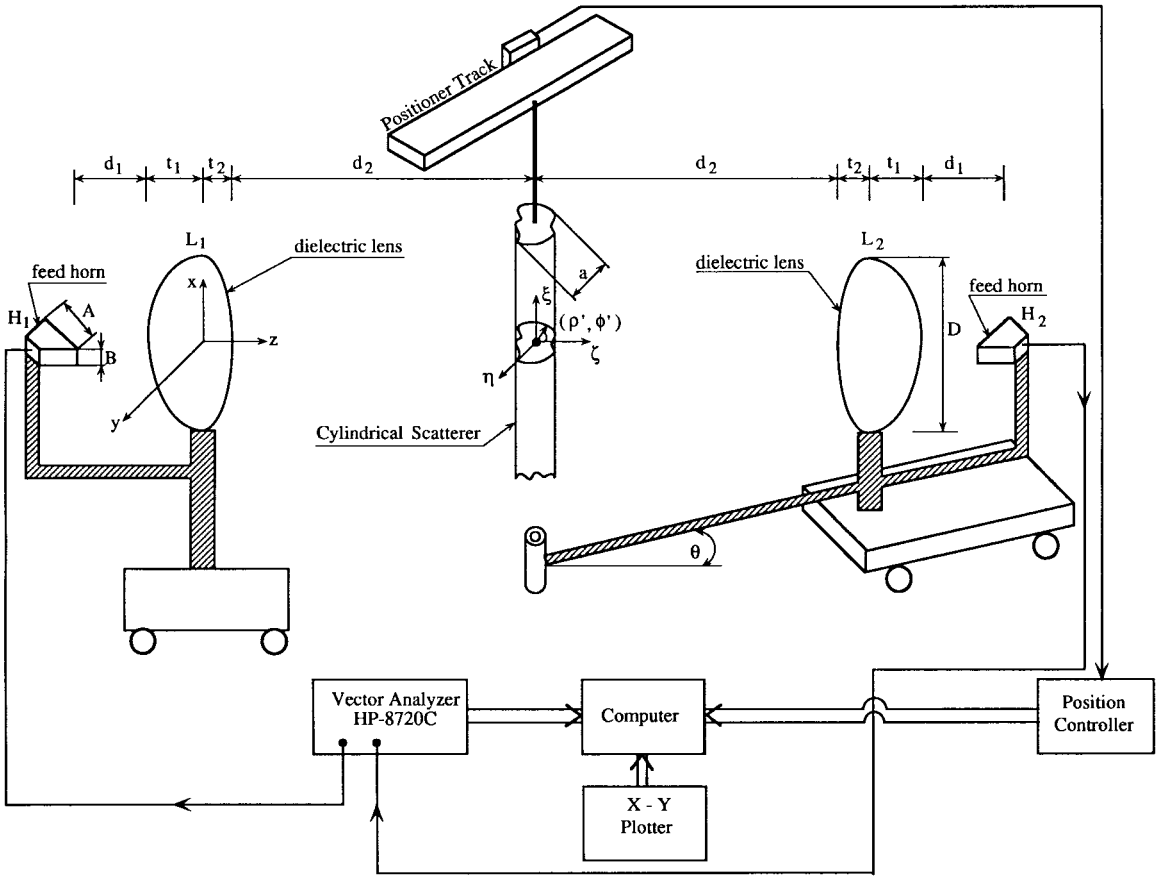

Fig. 1. Schematic configuration of the focused-beam system.

and $n = \sqrt{\varepsilon_r}$ is the refraction index of the lens material. In analogy to the analysis of thin dielectric lenses [4], we define for each lens an equivalent focal length f given by $1/f = 1/f_1 + 1/f_2$.

In this paper we made the assumption that the propagation mechanism of the focused beam system and the scattered field by the cylinder can be described by fundamental Gaussian beams. Goldsmith [5] has shown that feed horn radiation characteristics can be approximated by a fundamental Gaussian beam with minimum waists w_{0e} and w_{0h} representing the radiation in E and H planes. The waists w_{0e} and w_{0h} are related to the feed horn 10-dB beamwidths BW_e and BW_h by the approximate formula $w_{0e,h} = 0.68\lambda/BW_{e,h}$. The feed horn was designed such that w_{0e} and w_{0h} are close in value. Accordingly, we can define an equivalent quasi-circular minimum waist of the feed horn by $w_{0f} = \sqrt{w_{0e}\, w_{0h}}$. In addition, we made the assumption [4] that the two lenses act as phase transformers, each providing a phase advancement approximately proportional to the square of the distance r of a ray from the axis of propagation:

$$\Delta\phi = \pi r^2/\lambda f. \tag{3}$$

This phase advancement transforms the diverging Gaussian beam of H_1 feed horn (see Fig. 1) to a converging Gaussian beam with minimum waist of w_{0l}, located a distance d_2 from the lens surface. By symmetry, this converging Gaussian beam is transformed into an outward Gaussian beam captured by the second lens and transformed into an inward Gaussian beam captured by H_2 feed horn as shown in Fig. 1. Accordingly, at half the distance between the lenses, we obtain a minimum Gaussian beam waist w_{0l} with constant phase distribution. The system is initially calibrated before the cylinder movement, then the cylinder is mounted on a positioner track and moved along a line perpendicular to the focused beam axis. The position of the cylinder along the y axis and the relative amplitude $\Delta\alpha$ and phase $\Delta\phi$ of the received signal $R(y) = \Delta\alpha e^{j\Delta\phi}$ are recorded. The recorded signal is referenced to the value without the cylindrical scatterer.

A. System Analysis Without the Scatterer

The total loss is proportional to the coupling between the Gaussian beams involved. Due to the symmetry of the system around its center-line, we can simplify the computation by considering only the left half of the system and square the result (double in decibels). The coupling between the Gaussian beams on the two opposite sides of L_1 lens will be computed on the lens interface plane. The electric field distribution on this plane can be described by [5]

$$E = E_0\, e^{-(r^2/w^2)}\, e^{j(\pi r^2/\lambda R)} \tag{4}$$

where

$$w = w_0\left[1 + \left(\frac{\lambda z}{\pi w_0^2}\right)^2\right]^{1/2} \tag{5}$$

and

$$R = z\left[1 + \left(\frac{\pi w_0^2}{\lambda z}\right)^2\right] \tag{6}$$

in which w is the waist and R is the radius of curvature of the Gaussian beam on the lens surface. w_0 is the minimum waist of the Gaussian beam and z is the distance from the minimum waist location to the lens surface. E_0 is a normalization factor. We denote w_f, R_f, w_{0f}, d_1, and E_{0f} the corresponding parameters of the left (feed horn H_1) Gaussian beam and w_l, R_l, w_{0l}, d_2, and E_{0l} the right Gaussian beam parameters. The right Gaussian beam goes through a phase transformation given by (3) on the lens aperture plane and without any change beyond its extent. The coupling factor, C_{lf} between the two Gaussian beams is derived from a two-dimensional integral over the electric field distribution of the two beams [5]

$$C_{lf} = \int_0^{\infty}\int_0^{2\pi} E_l E_f^* \, r \, dr \, d\phi. \tag{7}$$

If the integral is carried out in two parts, on the lens aperture of diameter D and beyond it, we find

$$C_{lf} = \frac{2}{w_f w_l}\left[\frac{1 - e^{-\alpha(D^2/4)}}{\alpha} + \frac{e^{-\beta(D^2/4)}}{\beta}\right] \tag{8}$$

in which

$$\alpha = \frac{1}{w_f^2} + \frac{1}{w_l^2} + j\frac{\pi}{\lambda}\left(\frac{1}{f} - \frac{1}{R_l} - \frac{1}{R_f}\right) \tag{9}$$

and

$$\beta = \frac{1}{w_f^2} + \frac{1}{w_l^2} - j\frac{\pi}{\lambda}\left(\frac{1}{R_l} + \frac{1}{R_f}\right). \tag{10}$$

One can observe that for $D \to \infty$, $R_f = f_1$, $R_l = f_2$, and $w_l = w_f$ the coupling factor $C_{lf} = 1$ as expected from geometrical optics considerations. Thus, if the electric field intensity transmitted by H_1 feed horn is E_{0f} the total electric field received by H_2 feed horn would be $E_{0f}C_{lf}^2$.

B. System Analysis with the Scatterer

In this case the total electric field received by H_2 feed horn is the superposition of the electric field without the scatterer and the electric field scattered from the arbitrarily cross-section cylinder illuminated by a Gaussian beam with circular cross-section and minimum waist w_{0l}.

The forward-scattered field by the cylinder E_{sj} can be expressed in terms of the induced axial surface current density J_{sx} on the cylinder periphery and the incident electric field E_{inc} [1]

$$E_{sj} = -j\frac{Z_0}{2\lambda}E_{\text{inc}}\oint_{s_1} J_{sx}\, e^{jk\rho' \sin\phi'}\, dl \tag{11}$$

in which $Z_0 = 120\pi$ and S_1 is the line contour defining the cylinder's periphery with local coordinates (ρ', ϕ'). We can express E_{inc} in terms of the electric field intensity transmitted by H_1 feed horn, E_{0f} the coupling coefficient, C_{lf} on the interface plane of L_1 lens given by (7), and η_{inc} the ratio of the amount of energy captured by the cylinder to the entire energy passing through the cylinder's incident plane, such that $E_{\text{inc}} = E_{0f}C_{lf}\sqrt{\eta_{\text{inc}}}$. We can compute η_{inc} by

$$\eta_{\text{inc}} = \frac{\displaystyle\int_0^{\infty}\int_0^{a/2} e^{-2[(x^2+y^2)/w_{0l}^2]}\, dx\, dy}{\displaystyle\int_0^{\infty}\int_0^{\infty} e^{-2[(x^2+y^2)/w_{0l}^2]}\, dx\, dy} = 1 - erffc\left(\frac{a}{\sqrt{2}w_{0l}}\right) \tag{12}$$

in which a is the cylinder's projected width on the incident field plane.

In the proposed model we make the assumption that the scattered electric field can be approximated by an elliptical cross-section Gaussian beam with minimum waists $w_{0jx} = w_{0l}$ on x axis (infinite extent cylinder) and $w_{0jy} = w_{0j} = \alpha_j \cdot a$ on y axis. α_j is a proportionality coefficient between the shadow width of the cylinder a and the minimum waist of the equivalent Gaussian beam of the scattered electric field w_{0j}. A. G. van Nie [6] has shown that the Gaussian mode solution to the wave equation holds for $w_0 \geq \lambda/2$. This bound may impose a restriction on the minimum cylinder's width to comply with the Gaussian beam model of the scatterer as described later. Consequently, the electric field distribution of the scattered field on the interface plane of L_2 lens can be described by

$$E_{pj} = E_{sj}\, e^{-(x^2/w_{jx}^2 + y^2/w_{jy}^2)}\, e^{j(\pi/\lambda)(x^2/R_{jx} + y^2/R_{jy})} \tag{13}$$

in which w_{jx}, w_{jy} are the x- and y-scattered field waists on the interface plane computed by (5) with $w_{0jx} = w_{0l}$, $w_{0jy} = w_{0j}$ and R_{jx}, R_{jy} are the corresponding x and y radii of curvature computed by (6) with $z = d_2$. E_{sj} is given by (11). This field distribution goes through a phase transformation given by (3) and is coupled with the field distribution of H_2 feed horn given by (4) with $w = w_f$, $R = R_f$, $w_0 = w_{0f}$, and $z = d_1$. Computation of the coupling coefficient by (7) with the double integration performed on the lens aperture and beyond yields

$$C_{jf} = \frac{2}{\pi w_f\sqrt{w_{jx}w_{jy}}} \cdot\left\{\int_0^{\pi}\left[\frac{1 - e^{-(D^2/4)(\alpha_{jx}\cos^2\phi + \alpha_{jy}\sin^2\phi)}}{(\alpha_{jx}\cos^2\phi + \alpha_{jy}\sin^2\phi)} + \frac{e^{-(D^2/4)(\beta_{jx}\cos^2\phi + \beta_{jy}\sin^2\phi)}}{(\beta_{jx}\cos^2\phi + \beta_{jy}\sin^2\phi)}\right] d\phi\right\} \tag{14}$$

where

$$\alpha_{jx} = \frac{1}{w_{jx}^2} + \frac{1}{w_f^2} + j\frac{\pi}{\lambda}\left(\frac{1}{f} - \frac{1}{R_{jx}} - \frac{1}{R_f}\right) \tag{15}$$

$$\alpha_{jy} = \frac{1}{w_{jy}^2} + \frac{1}{w_f^2} + j\frac{\pi}{\lambda}\left(\frac{1}{f} - \frac{1}{R_{jy}} - \frac{1}{R_f}\right) \tag{16}$$

$$\beta_{jx} = \frac{1}{w_{jx}^2} + \frac{1}{w_f^2} - j\frac{\pi}{\lambda}\left(\frac{1}{R_{jx}} + \frac{1}{R_f}\right) \tag{17}$$

$$\beta_{jy} = \frac{1}{w_{jy}^2} + \frac{1}{w_f^2} - j\frac{\pi}{\lambda}\left(\frac{1}{R_{jy}} + \frac{1}{R_f}\right). \tag{18}$$

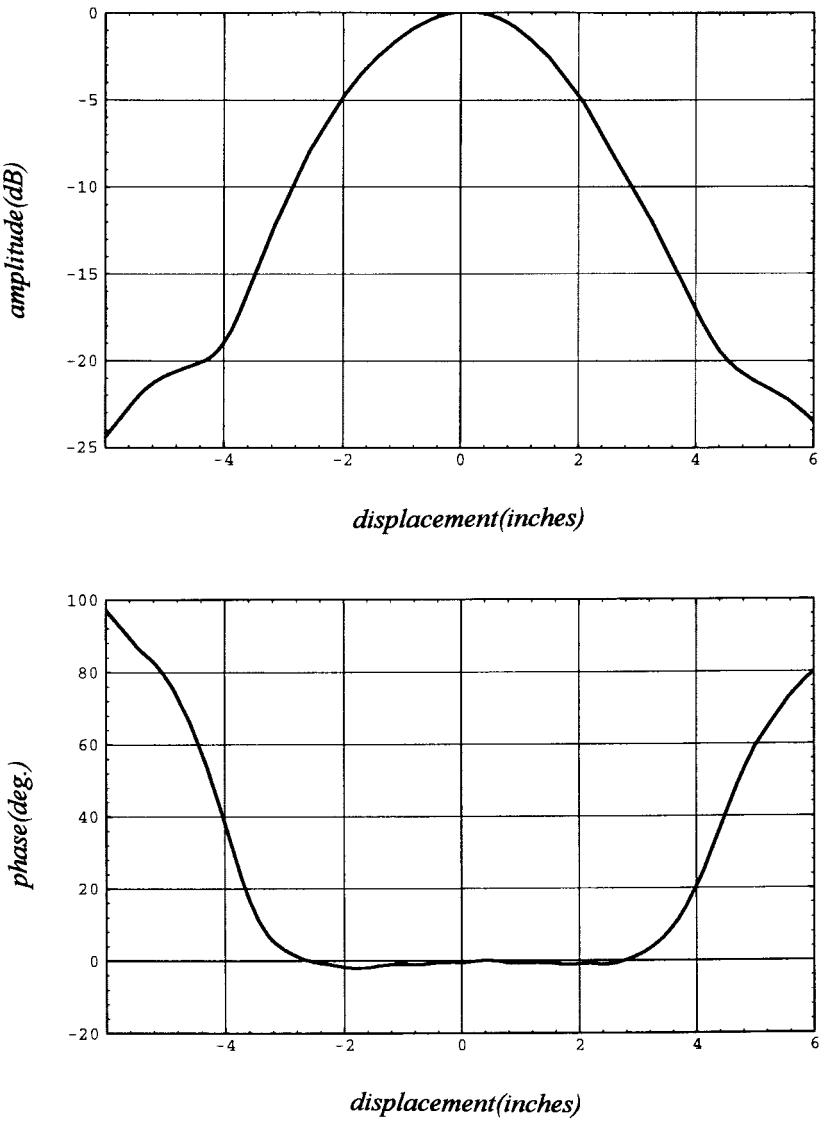

Fig. 2. Typical near-field recorded signal (amplitude and phase) at the minimum waist location in the focal plane ($d_2 = 65$ in, vertical polarization, $f = 12$ GHz).

Consequently, the scattered electric field, E_{scat} received by H_2 feed horn is

$$E_{\text{scat}} = -\frac{Z_0}{2\lambda} E_{0f} C_{lf} C_{jf} \sqrt{\eta_{\text{inc}}} \oint_{s_1} J_{sx}\, e^{jk\rho' \sin\phi'}\, dl. \quad (19)$$

The induced field ratio (IFR) is defined as the ratio of the forward-scattered field to the hypothetical field radiated in the forward direction by a plane wave in the reference aperture of width equal to the shadow of the geometrical cross section of the cylinder on the incident plane wavefront [1]. Thus the IFR for an incident electric field with intensity, E_0, and parallel to the cylinder axis is given by

$$\text{IFR} = -\frac{Z_0}{2aE_0} \oint_{S_1} J_{sx}\, e^{jk\rho' \sin\phi'}\, dl. \quad (20)$$

The IFR is defined for an incident *plane wave* (constant in phase and amplitude), while in a focused-beam system the incident field is quasi-planar (constant in phase and Gaussian in amplitude). The implication would be a different axial component of the induced surface current density, J_{sx} in the case of Gaussian beam illumination. The proportionality coefficient α_j bridges over the difference between the two integrals such that we can substitute (20) into (19) to obtain

$$E_{\text{scat}} = \frac{a}{\lambda} E_{0f} C_{lf} C_{jf} \sqrt{\eta_{\text{inc}}}\ \text{IFR}. \quad (21)$$

Accordingly, the total electric field received by H_2 feed horn in the presence of the cylinder is

$$E_{\text{total}} = E_{0f} C_{lf}^2 \left[1 + \frac{a}{\lambda} \frac{C_{jf}}{C_{lf}} \sqrt{\eta_{\text{inc}}}\ \text{IFR}\right]. \quad (22)$$

The recorded signal $R(y)$ in the focused-beam system is referenced to the signal received by H_2 feed horn without the cylinder presence, $E_{0f} C_{lf}^2$. Therefore, if the change in amplitude when the cylinder crosses the system axis is denoted by $\Delta\alpha$ (decibels) and the change in phase by $\Delta\phi$, we can

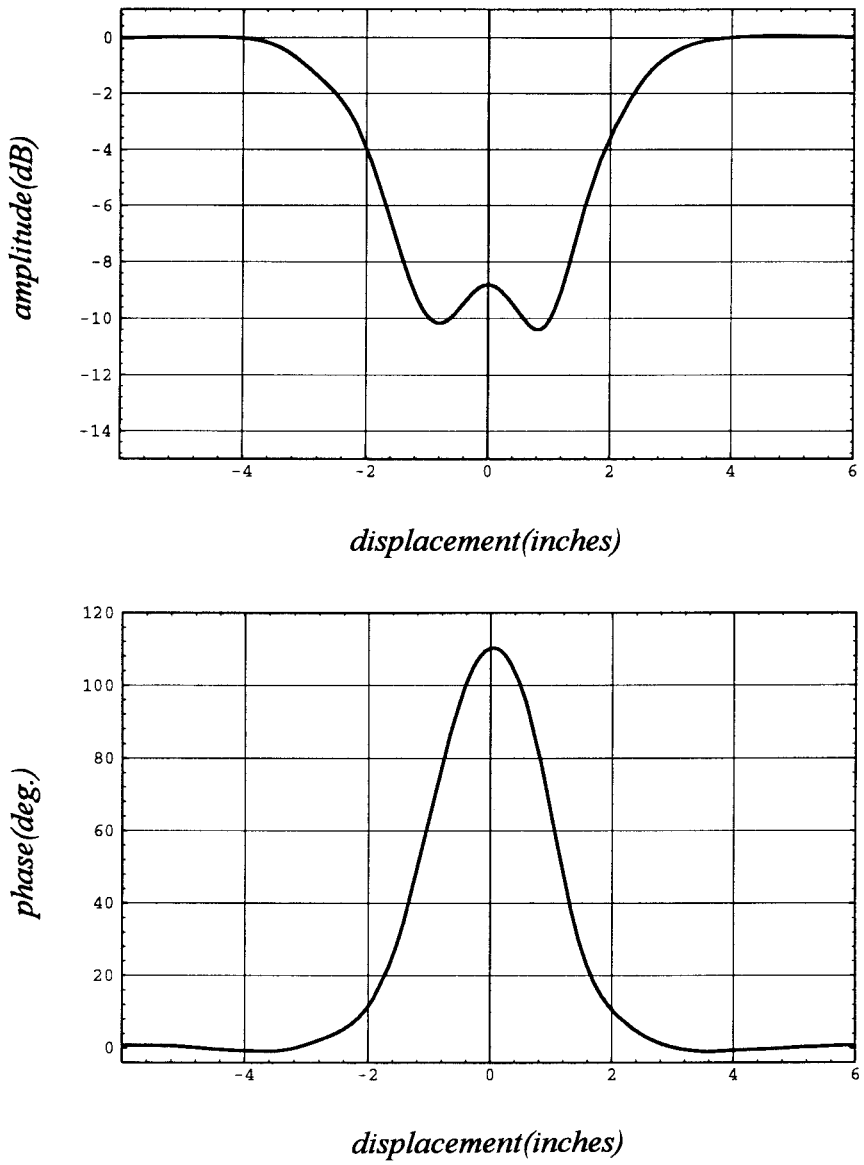

Fig. 3. Typical recorded signal (amplitude and phase) by H_2 feed horn throughout the plastic beam movement ($a = 2.25$ in, vertical polarization, $f = 12$ GHz).

express the IFR by

$$\text{IFR} = (10^{\Delta\alpha/20}\, e^{j\Delta\phi} - 1)\frac{1}{\frac{a}{\lambda}\frac{C_{jf}}{C_{if}}\sqrt{\eta_{\text{inc}}}}. \tag{23}$$

In addition, we can use the system shown in Fig. 1 to measure the scattering pattern of the cylinder. We move the lens L_2 and the feed horn H_2 on an arch with radius d_2 and record the angular (θ) dependence of the received signals (amplitude and phase) by the H_2 feed horn with and without the tested cylindrical scatterer. Subtraction of these two signals is proportional to the scattering pattern of the cylinder. The subtraction operation can be performed by a computer after the measurement or in real time by inserting an automatic null-balance branch, mainly consisting of a computer control digital phase shifter and attenuator, to cancel the signal without the scatterer. In the real-time option, the dynamic range of the pattern will increase.

III. Numerical Results

A focused-beam system was designed and built. AEL antenna horn model H-1498 operating in the frequency range 2–18 Ghz was chosen as feed. The horn has almost a constant 10-dB beamwidth in both E and H planes over the entire frequency bandwidth. Based on the beamwidth data the equivalent feed horn Gaussian beam minimum waists, w_{0e} and w_{0h} were computed. The diameter of the lens was chosen to be 22 in and it was manufactured from material with dielectric constant 2.3. The lens focal distances f_1 and f_2 were chosen as 21 and 80 in, respectively. Due to the finite-diameter of the lens and the variation of the feed horn phase center location with frequency, we had to determine d_2 for each test frequency. This task was accomplished by probing the amplitude and phase of the electric field in front of L_1 lens. The distance d_2 was chosen as the distance for which the maximum phase flatness was obtained. Fig. 2 shows a typical recorded near-field signal (amplitude and phase) at the

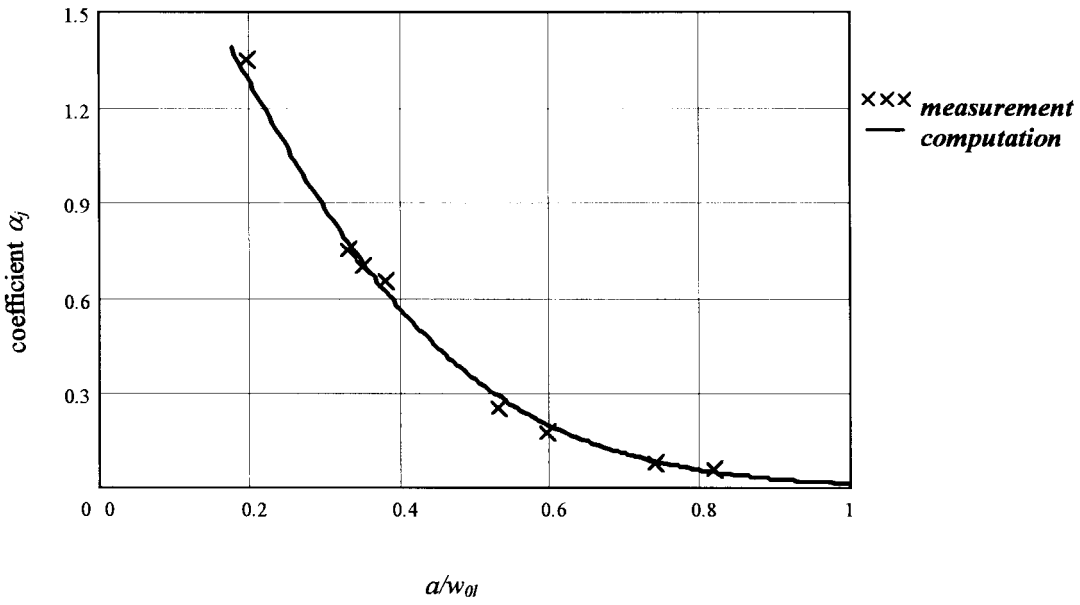

Fig. 4. Dependence of the proportionality coefficient α_j on a/w_{0l}.

TABLE I
COMPARISON OF THE IFR MEASURED WITH THE FOCUSED-BEAM SYSTEM AND COMPUTED VALUES BY MOM AND FEM, FOR THE VARIOUS TYPES OF CYLINDERS CONSIDERED

	Vertical Polarization				Horizontal Polarization			
	IFR amplitude		*IFR* phase (deg.)		*IFR* amplitude		*IFR* phase (deg.)	
Cyl. type	MoM/FEM	Focused Beam	MoM/FEM	Focused Beam	MoM/FEM	Focused Beam	MoM/FEM	Focused Beam
Metal circ. *a=0.375"*	1.63	1.53	151.2	156.1	0.66	0.73	-145.1	-128.7
Plastic rect. *a=0.476"*	2.24	2.28	164.3	165.5	1.05	0.99	125.9	129.1
Plastic rect. *a=2.25"*	1.91	1.93	158.8	163.0	1.79	1.79	162.6	167.4
Metal rect. *a=0.54"*	2.42	2.46	151.8	152.3	1.2	1.04	-165.3	-144.0
Metal rect. *a=2.03"*	1.14	1.11	172.6	172.6	0.98	1.11	-176.6	179.2

minimum waist location for 12 GHz as operating frequency and vertical polarization. The abscissa represents the relative distance along the y axis in front of L_1 lens. One can observe the Gaussian amplitude tapering and the phase flatness of the probed electric field. In this case the distance, d_1 from the feed horn to the lens was found to be 19.375 in and the distance d_2 from the probe to the lens was 65 in. The minimum waist size, w_{0l} was measured to be 2.75 in at the -8.7-dB point from the value measured on the system axis. The losses between the two feed horns were measured and found to be -10 dB. Computation of the losses based on (8) yields -9.6 dB. This experiment validated the assumption that the internal fields between the lenses can be approximated by fundamental Gaussian beams.

Three cylinders—a metallic circular rod 0.375-in diameter, a rectangular metal beam 0.54 $\times$ 2.033 in, and a plastic beam 0.476 $\times$ 2.25 in with $\varepsilon_r = 5.0$—were tested at three frequencies 4, 8, and 12 GHz for both vertical (VP) and horizontal (HP) incident field polarizations. The rectangular beams were tested for incident fields on the narrow and on the broadside. Fig. 3 shows a typical recorded signal (amplitude and phase) throughout the plastic beam movement between the two lenses for vertical polarization and 12-GHz operating frequency. The plastic beam was illuminated on its broadside, $a = 2.25$ in. The abscissa is proportional to the relative position of the cylinder from the center axis of the system. The maximum perturbation in amplitude and phase throughout the beam movement occurs when the beam crosses the center axis.

The data from all measurements was processed and the IFR was computed based on (23) and compared to the IFR values computed analytically in the case of the metallic rod, by the method of moments (MoM) for the metallic rectangular beam and by finite elements (FEM) for the plastic beam. Based on this comparison we have been able to establish a general curve of the dependence of the proportionality coefficient α_j on the ratio of a/w_{0l}. This dependence is shown in Fig. 4. Curve fitting of the coefficient α_j based on the measurement data

(crossed points) results in the function $\alpha_j = 2e^{-5(a/w_{0l})^{3/2}}$ (solid line). One can observe that increase in a/w_{0l} causes a decrease in the coefficient α_j. As expected, the increased tapering of the incident wave along the cylinder's cross section, causes a net reduction effect on the effective size of the equivalent Gaussian beam scattered field minimum waist, w_{0jy}. Moreover, a large ratio of $a/w_{0l}\,(>1)$ may cause a large error in the estimate of the coefficient α_j, due to the relatively small slope of the graph in this range. Practically, for an acceptable error (less than 10%) in the IFR value, the measurement can be performed for cylinders in the range of $0.2 < a/w_{0l} < 1$. In addition, the lower bound is determined by the validity of the Gaussian beam model adopted in this paper, $a > \lambda/2$. Computation results of the IFR for the various types of cylinders compared to the computed values by MoM and FEM at 12 GHz are shown in Table I. One can observe a nice agreement between the numerical computation and the computed values in the focused beam system. The IFR values of the circular metallic cylinder are slightly off from the values computed by MoM/FEM. This deviation can be attributed to the relatively narrow diameter of the cylinder (0.38λ), which does not meet the criterion of the Gaussian model.

IV. Summary

A new procedure for the scattering analysis of arbitrarily shaped cylinders have been presented. The method is based on a focused-beam system. The analysis is based on the assumption that the electric fields between the lenses and the scattered field from the cylinder can be described by fundamental Gaussian beams. A quasi-empirical proportionality coefficient between the physical projected width of the cylinder and the equivalent Gaussian beam scattered field minimum waist was determined for the IFR computation, and a general graph was generated. Computation of the coupling between the Gaussian beams in the system and measurement of the change in amplitude and phase of the received signal enabled computation of the IFR values of different type of cylinders. The agreement between the computed values by numerical techniques such as MoM and FEM and the values computed from measurements in the focused-beam system verify well. The new method complements Rusch's method, which determines only the IFR value, based on far-field measurement in an open system. Rusch's procedure may encounter measurements errors from reflections and multiple interactions between the scatterer and the transmitting and receiving antennas. These errors are eliminated in the focused beam system, due to the nature of the system. The information obtained on the scattering pattern helps to refine the calculations of the scattering analysis of large-space frame radomes.

Acknowledgment

The authors wish to express their thanks to J. Sangiolo and A. Mantz for very helpful and fruitful discussions and to C. Slotta for performing the measurements during the course of this work. All are associated with ESSCO, Concord, MA.

References

[1] W. V. T. Rusch, J. A. Hansen, C. A. Klein, and R. Mittra, "Forward scattering from square cylinders in the resonance region with application to aperture blockage," *IEEE Trans. Antennas Propagat.*, vol. AP-24, pp. 182–189, Mar. 1976.

[2] R. Shavit, A. Cohen, and E. C. Ngai, "Characterization of the scattering parameters from arbitrary shaped cylinders by near-field probing," *IEEE Trans. Antennas Propagat.*, vol. 43, pp. 1–5, June 1995.

[3] Y. T. Lo and S. W. Lee, *Antenna Handbook: Theory, Applications, and Design.* New York: Van Nostrand Reinhold, 1988, pp. 16-9–16-11.

[4] J. W. Goodman, *Introduction to Fourier Optics.* New York: McGraw-Hill, 1968, pp. 77–97.

[5] P. F. Goldsmith, *Infrared and Millimeter Waves.* New York: Academic, 1982, ch. 5.

[6] A. G. van Nie, "Rigorous calculation of the electromagnetic field of wave beams," *Philips Tech. Rev.*, vol. 19, pp. 378–394, 1964.

Reuven Shavit (M'82–SM'90) was born in Rumania on November 14, 1949. He received the B.S. and M.S. degrees in electrical engineering from the Technion, Israel, in 1971 and 1977, respectively, and the Ph.D. degree in electrical engineering from the University of California, Los Angeles, in 1982.

From 1971 to 1993, he worked as a Staff Engineer and Antenna Group Leader in the Electronic Research Laboratories of the Israeli Ministry of Defense, Tel Aviv, where he was involved in the design of reflector, microstrip, and slot antenna arrays. He was also a part-time Lecturer at Tel Aviv University, teaching various antenna and electromagnetic courses. From 1988 to 1990, he was associated with ESSCO, Concord, MA, as a Principal Engineer involved in scattering analysis and tuning techniques of high-performance ground-based radomes. Currently, he is with Ben-Gurion University of the Negev as Lecturer doing research in microwave components and antennas. His present research interest is in the areas of tuning techniques for radomes and numerical methods for design microstrip, slot, and reflector antennas.

Tom Wells, photograph and biography not available at the time of publication.

Albert Cohen was born in Boston, MA, on October 14, 1927. He began his career directly after receiving the B.S. degree in electrical engineering from the Massachusetts Institute of Technology (MIT) in 1951. In 1964, he received the M.S. degree in engineering management from Northeastern University.

He joined Gabriel Laboratories and became Senior Research Engineer. In 1955, he joined the technical staff of MIT Lincoln Laboratory, progressing to Group Leader. In 1961, he cofounded Electronic Space Systems Corporation (ESSCO) of Concord, MA, a high-technology company specializing in the research, development, design, and manufacture of aerospace ground equipment. He became its President and Chief Executive Officer in 1964. Presently, he is Chairman of the Board of ESSCO Collins Ltd. in Ireland, ESSCO's manufacturing subsidiary in the European Common Market, and is a member of the Board of Directors of Unifirst Corporation. He has authored several articles for various technical journals. A representative paper, "A 150 Foot Metal Space Frame Radome," (WADC Tech. Rep. 57-314 ASTIA Document AD130929, vol. 1, June 1957), described the first utilization of metallic beams in a triangulated spherical large ground radome exhibiting extremely large bandwidth. This design concept was implemented as what is now known as the "Haystack Radome" and has been adopted worldwide in over 1000 applications.

Mr. Cohen has received a number of awards, is a Registered Professional Engineer in the Commonwealth of Massachusetts, and is member of several professional and technical societies.